

# IEICE Proceeding Series

Nonlinear dynamics in a photonic integrated circuit for fast chaos generation

Yasuhiro Akizawa, Rie Takahashi, Hiroki Aida, Taiki Yamazaki, Atsushi Uchida, Takahisa Harayama, Ken Tsuzuki, Satoshi Sunada, Kazuyuki Yoshimura, Ken-ichi Arai, Peter Davis

Vol. 1 pp. 134-137

Publication Date: 2014/03/17

Online ISSN: 2188-5079

Downloaded from [www.proceeding.ieice.org](http://www.proceeding.ieice.org)



## Nonlinear dynamics in a photonic integrated circuit for fast chaos generation

Yasuhiro Akizawa<sup>1</sup>, Rie Takahashi<sup>1</sup>, Hiroki Aida<sup>1</sup>, Taiki Yamazaki<sup>1</sup>, Atsushi Uchida<sup>1</sup>,  
Takahisa Harayama<sup>2,3</sup>, Ken Tsuzuki<sup>4</sup>, Satoshi Sunada<sup>2,5</sup>,  
Kazuyuki Yoshimura<sup>2</sup>, Ken-ichi Arai<sup>2</sup>, and Peter Davis<sup>2,6</sup>

<sup>1</sup>Department of Information and Computer Sciences, Saitama University,  
255 Shimo-Okubo, Sakura-ku, Saitama City, Saitama, 338-8570, Japan

<sup>2</sup>NTT Communication Science Laboratories, NTT Corporation,  
2-4 Hikaridai, Seika-cho, Soraku-gun, Kyoto, 619-0237, Japan

<sup>3</sup>Department of Mechanical Engineering, Toyo University,  
2100 Kujirai, Kawagoe, Saitama, 350-8585, Japan

<sup>4</sup>NTT Photonics Laboratories, NTT Corporation,  
3-1 Morinosatowakamiya, Atsugi, Kanagawa, 243-0198, Japan

<sup>5</sup>Institute of Science and Engineering, Kanazawa University,  
Kakuma-machi, Kanazawa, Ishikawa, 920-1192, Japan

<sup>6</sup>Telecognix Corporation,  
58-13 Shimooji-cho, Yoshida, Sakyo-ku, Kyoto, 606-8314, Japan  
Emails: {s11mm301, uchida}@mail.saitama-u.ac.jp

**Abstract**– We experimentally investigate nonlinear dynamics in a photonic integrated circuit consisting of a semiconductor laser, semiconductor optical amplifiers, a photodiode, and a short external cavity. We investigate two-dimensional bifurcation diagram when the injection current and the feedback power are simultaneously changed. We observe fast chaotic oscillation and intermittent dynamics in photonic integrated circuits with different external cavity lengths.

### 1. Introduction

Semiconductor lasers subject to optical feedback have rich nonlinear dynamics because they show bifurcation phenomena and generate chaotic laser intensity fluctuations, depending on the parameter values of an external cavity length, injection current, and feedback strength [1]. Chaotic lasers are promising for the application of fast random number generation at rates over 1 Gigabit per second (Gb/s), because of their fast irregular intensity fluctuations [2-12]. It has been theoretically guaranteed that chaotic lasers can be used for nondeterministic random bit generators [13]. There are a few reports on random number generation with a photonic integrated circuit (PIC). The PIC consists of a distributed-feedback (DFB) semiconductor laser, semiconductor optical amplifiers (SOAs), an external reflector at a distance of 10 mm, and a photodiode [8]. However, detail characteristics of nonlinear dynamics in a PIC with the external cavity length shorter than 10 mm have not been investigated yet in the literature [14].

In this study, we experimentally observe bifurcation phenomena of the laser intensity in a PIC. We create a two-dimensional bifurcation diagram when the normalized injection current and the feedback power are

changed for PICs with different external cavity lengths  $L$  ( $L = 2, 5,$  and  $10$  mm). We observe fast chaotic oscillations and intermittent dynamics in large parameter regions of these PICs.

### 2. Photonic integrated circuit for fast chaos generation

Figure 1(a) and (b) show the schematics of our PIC for fast chaos generation. The PIC consists of a semiconductor laser, two semiconductor optical amplifiers (SOA1 and SOA2), a photodiode, and an external cavity ( $L = 2, 5,$  and  $10$  mm). The PIC is similar to one which is used in Ref. [8], however, the different external cavity length of 5 mm is used in this experiment. The output of the semiconductor laser is amplified by SOA1 and SOA2. The amplified laser output is reflected by the external mirror (with HR coating) and re-injected into the semiconductor laser. The output of the semiconductor laser is detected by the photodiode and converted into an electronic signal. The injection current of the DFB laser is adjusted to generate chaos. The feedback strength is controlled by the injection currents of SOA1 and SOA2. The whole PIC is packaged within the size of  $10 \times 20$  mm.

Figure 2 shows our experimental setup for observation of nonlinear intensity dynamics. We used a bias tee to obtain AC component of the electronic signal of laser output. The electronic signal was amplified by an electronic signal amplifier and measured by a digital oscilloscope and a RF spectrum analyzer. We observed two-dimensional bifurcation diagram by changing two parameter values of the injection current ( $J/J_{th}$ ) normalized by the lasing threshold value and the ratio between the feedback power and the laser output power ( $P_f$ ). We used three PICs with different external cavity lengths ( $L = 2, 5,$

and 10 mm) in order to create two-dimensional bifurcation diagrams.

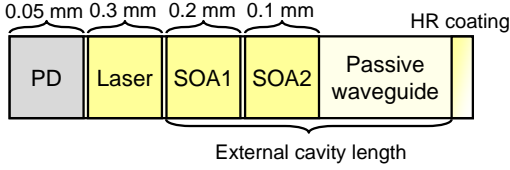


Fig. 1 Schematic diagram for the photonic integrated circuit. PD: photodiode, Laser: distributed-feedback semiconductor laser, SOA1 and SOA2: semiconductor optical amplifier 1 and 2, HR coating: high-reflection coating.

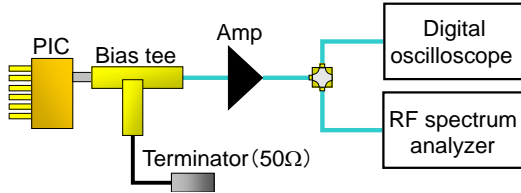


Fig. 2 Experimental setup for the observation of intensity dynamics. PIC: Photonic integrated circuit, Amp : electronic signal amplifier.

### 3. Experimental result

#### 3.1. Temporal waveforms and RF spectra

Figure 3 shows the temporal waveforms and the corresponding RF spectra observed in the PIC with the external cavity length of 5 mm. The outputs of the PIC show various types of intensity dynamics and bifurcations for different parameter values of  $J/J_{th}$  and  $P_f$ . Figures 3(a) and 3(g) show the temporal waveform and the RF spectrum for stable emission. The RF spectrum in Fig. 3(g) shows noise floor level. Figures 3(b) and 3(h) show the temporal waveform and the RF spectrum of a periodic state. The temporal waveform shows a periodic oscillation in Fig. 3(b) and the RF spectrum has a sharp peak in Fig. 3(h). Figures 3(c) and 3(i) correspond to a quasi-periodic state. The temporal waveform shows fast and slow oscillations in Fig. 3(c), and the RF spectrum has two peaks at around 0.60 and 6.48 GHz in Fig. 3(i). Figures 3(d) and 3(j) correspond to a chaotic state. Fast chaos generation can be achieved with the peak frequencies of the RF spectrum of 6.60 GHz, as shown in Fig. 3(j). Figures 3(e) and 3(k) show an intermittency state. The temporal waveform of the intermittency state in Fig. 3(e) consists of chaotic bursts and laminar states. The intermittent dynamics observed in this circuit range from tens of kHz to hundreds of MHz. Moreover, the temporal waveform of the intermittency dynamics in Fig. 3(i) is different from typical low-frequency fluctuations (LFFs), where sudden power dropout and gradual power recovery are found [15]. Figures 3(f) and 3(l) show a pulse-package state [16]. The frequency of fast pulsing oscillations shown in Fig. 3(f) corresponds to the external cavity frequency of 7.00 GHz, as shown in Fig. 3(l). Similar

dynamics shown in Fig. 3 can be observed in PICs with different external cavity lengths.

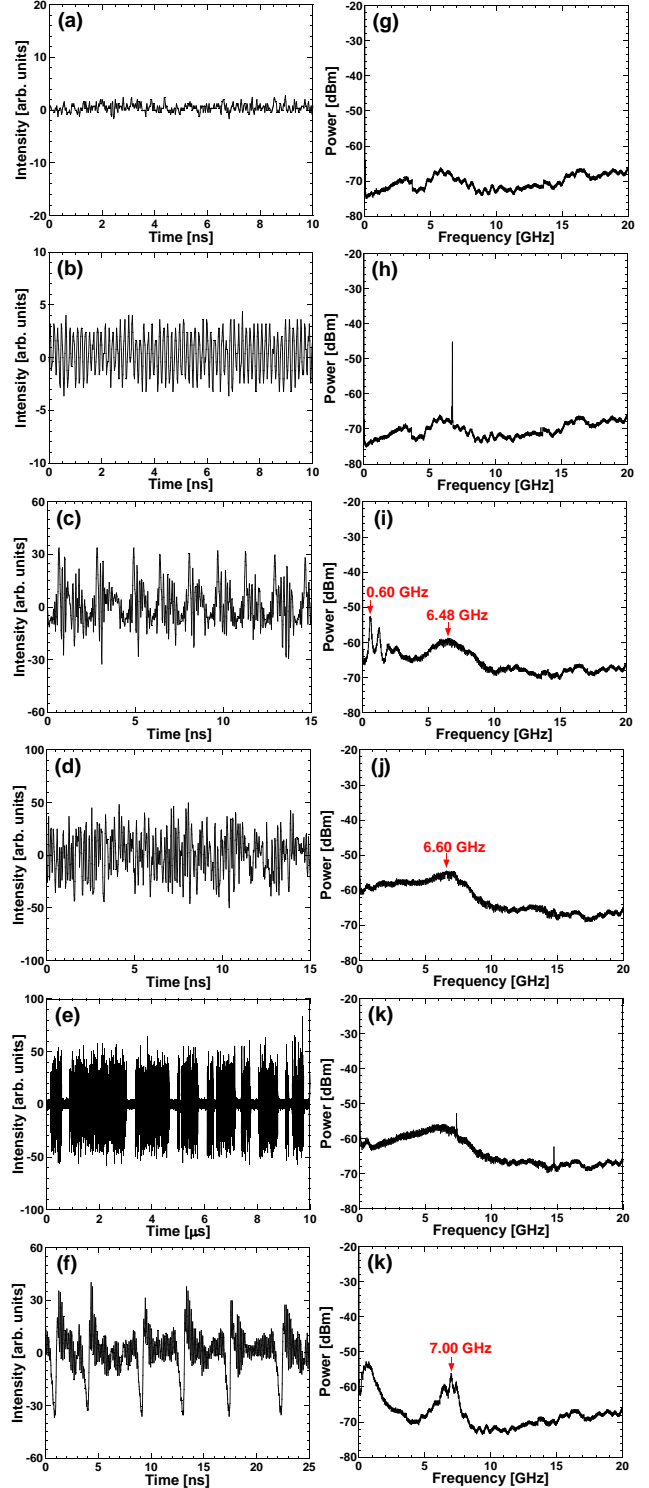


Fig. 3 (a)-(f) Temporal waveforms and (g)-(k) RF spectra. (a), (g) stable state ( $J/J_{th} = 1.20$ ,  $P_f = 0.021$ ), (b), (h) periodic state ( $J/J_{th} = 1.20$ ,  $P_f = 0.062$ ), (c), (i) quasi-periodic state ( $J/J_{th} = 5.00$ ,  $P_f = 0.015$ ), (d), (j) chaotic state ( $J/J_{th} = 3.40$ ,  $P_f = 0.110$ ), (e), (k) intermittency state ( $J/J_{th} = 3.40$ ,  $P_f = 0.086$ ), (f), (l) pulse package state ( $J/J_{th} = 1.50$ ,  $P_f = 0.083$ ).

### 3.2. Two-dimensional bifurcation diagrams

We created the two-dimensional bifurcation diagrams for PICs with the external cavity length of  $L = 2, 5,$  and  $10$  mm by changing  $J/J_{th}$  and  $P_f$ .

Figure 4 shows the two-dimensional diagram of the PIC with the external cavity length of  $10$  mm. Different colors in these diagrams indicate different dynamical states, such as no oscillation (dark gray), stable state (S, light gray), periodic state (P, greenish yellow), quasi-periodic state (QP, light blue), chaotic state (C, red), intermittency state (yellow), pulse-package state (PP, purple), and irregular pulsation state (orange). There are three large regions, quasi-periodic state (QP), chaos (C) and pulse package (PP). PP is dominant for low injection currents and large feedback strength (e.g.,  $J/J_{th} < 2$  and  $P_f > 0.03$ ). On the contrary, QP is observed for high injection currents and low feedback strengths ( $J/J_{th} > 4$  and  $P_f < 0.12$ ). Fast chaotic state (C) is observed for middle injection currents. For moderate injection currents and moderate feedback strengths ( $J/J_{th} \sim 2$  and  $P_f < 0.06$ ), intermittency state appears. In the intermittency regions, the bifurcation between intermittency and chaos is repeated as the feedback strength  $P_f$  is increased. This repetition is the characteristic dynamics for PICs.

Figure 5 shows the two-dimensional bifurcation diagram of the PIC with the external cavity length of  $5$  mm. The alphabets (a)-(f) in Fig. 5 correspond to the temporal dynamics shown in Fig. 3. This diagram also has major three regions such as QP, C and PP, as in Fig. 4. However, yellow intermittency islands fully spread in the wide parameter regions, compared with Fig. 4.

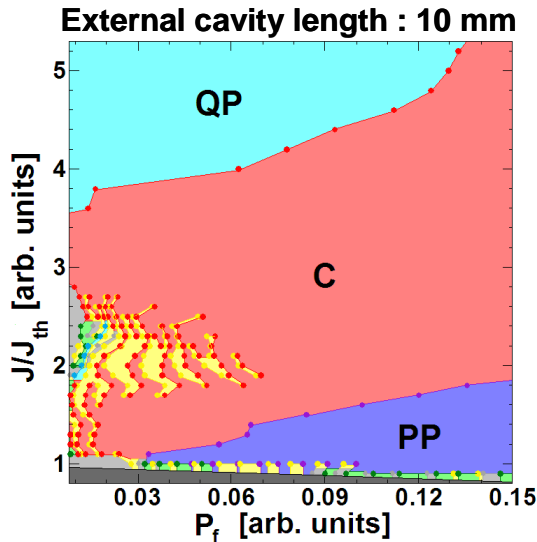


Fig. 4 Two-dimensional bifurcation diagram of the PIC with the external cavity length of  $10$  mm. Dark gray: no oscillation, light gray: stable state, greenish yellow: periodic state, light blue: quasi-periodic state (QP), red: chaos (C), yellow: intermittency, purple: pulse package (PP).

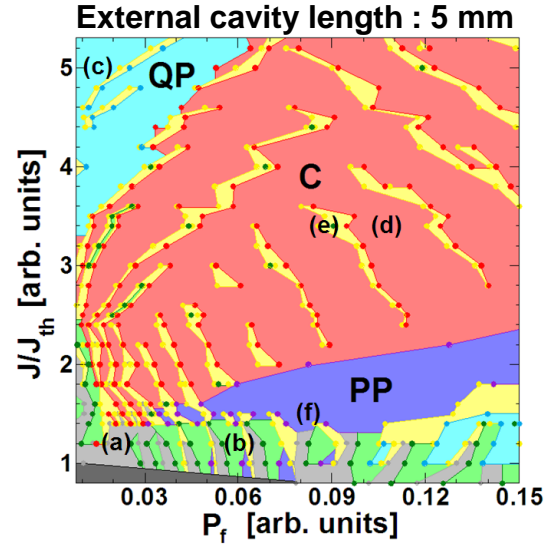


Fig. 5 Two-dimensional bifurcation diagram of the PIC with the external cavity length of  $5$  mm. Dark gray: no oscillation, light gray: stable state, greenish yellow: periodic state, light blue: quasi-periodic state (QP), red: chaos (C), yellow: intermittency, purple: pulse package (PP). The alphabets (a)-(f) correspond to the temporal dynamics shown in Fig. 3.

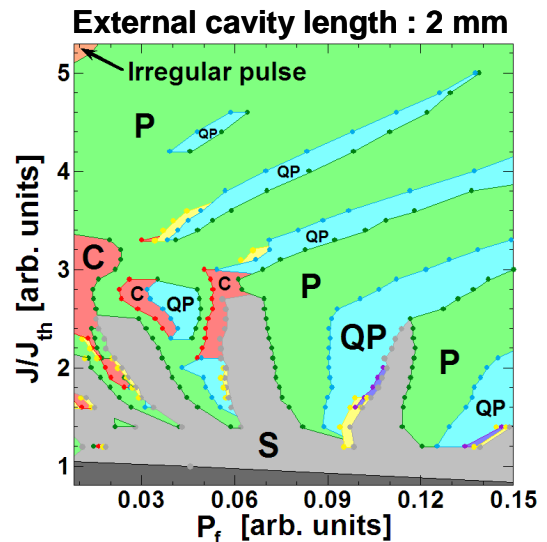


Fig. 6 Two-dimensional bifurcation diagram of the PIC with the external cavity length of  $2$  mm. Dark gray: no oscillation, light gray: stable state, greenish yellow: periodic state, light blue: quasi-periodic state (QP), red: chaos (C), yellow: intermittency, purple: pulse package (PP), orange: irregular pulsation.

Figure 6 shows the two-dimensional diagram of the PIC with the external cavity length of 2 mm. Periodic (P) and stable (S) regions are dominant and chaos (C) region is located in small regions in Fig. 6, unlike Figs. 4 and 5. We found that photonic integrated circuits with shorter external cavity length show smaller chaotic region in the two-dimensional bifurcation diagrams.

#### 4. Conclusion

We have investigated nonlinear dynamics in photonic integrated circuits with different cavity lengths of 2, 5, and 10 mm. We have investigated two-dimensional bifurcation diagram of the photonic integrated circuits when the injection current and the feedback strength are simultaneously changed. Quasiperiodicity, Chaos, and Pulse-package states were widely observed in the parameter regions. We observed the repetition of the bifurcation structure between chaos and intermittency. We found that photonic integrated circuits with shorter external cavity lengths have smaller chaos regions in the two-dimensional bifurcation diagrams. These results could be useful for random number generation using photonic integrated circuits for fast chaos generation [17].

#### Acknowledgments

We acknowledge support from Grant-in-Aid for Young Scientists and Management Expenses Grants from the Ministry of Education, Culture, Sports, Science and Technology in Japan.

#### References

[1] R. Lang and K. Kobayashi, "External Optical Feedback Effects on Semiconductor Injection Laser Properties," *IEEE Journal of Quantum Electronics*, Vol. 16, No. 3, pp. 347-355 (1980).  
 [2] A. Uchida, K. Amano, M. Inoue, K. Hirano, S. Naito, H. Someya, I. Oowada, T. Kurashige, M. Shiki, S. Yoshimori, K. Yoshimura, and P. Davis, "Fast physical random bit generation with chaotic semiconductor lasers," *Nature Photonics*, Vol. 2, No. 12, pp. 728-732 (2008).  
 [3] I. Reidler, Y. Aviad, M. Rosenbluh, and I. Kanter, "Ultrahigh-speed random number generation based on a chaotic semiconductor laser," *Physical Review Letters*, Vol. 103, No. 2, pp. 024102-1-4 (2009).  
 [4] I. Kanter, Y. Aviad, I. Reidler, E. Cohen, and M. Rosenbluh, "An optical ultrafast random bit generator," *Nature Photonics*, Vol. 4, pp. 58-61 (2010).  
 [5] K. Hirano, T. Yamazaki, S. Morikatsu, H. Okumura, H. Aida, A. Uchida, S. Yoshimori, K. Yoshimura, T. Harayama, and P. Davis, "Fast random bit generation with bandwidth-enhanced chaos in semiconductor lasers," *Optics Express*, Vol. 18, No. 6, pp. 5512-5524 (2010).

[6] A. Argyris, S. Deligiannidis, E. Pikasis, A. Bogris, and D. Syvridis, "Implementation of 140 Gb/s true random bit generator based on a chaotic photonic integrated circuit," *Optics Express*, Vol. 18, No. 18, pp. 18763-18768 (2010).  
 [7] P. Li, Y. C. Wang, and J. Z. Zhang, "All-optical fast random number generator," *Optics Express*, Vol. 18, No. 19, pp. 20360-20369 (2010).  
 [8] T. Harayama, S. Sunada, K. Yoshimura, P. Davis, K. Tsuzuki, and A. Uchida, "Fast nondeterministic random-bit generation using on-chip chaos lasers," *Physical Review A*, Vol. 83, No. 3, pp. 031803-1-4 (2011).  
 [9] N. Oliver, M. C. Soriano, D. W. Sukow, and I. Fischer, "Dynamics of a semiconductor laser with polarization-rotated feedback and its utilization for random bit generation," *Optics Letters*, Vol. 36, No. 23, pp. 4632-4634 (2011).  
 [10] P. Li, Y. Wang, A. Wang, L. Yang, M. Zhang, and J. Zhang, "Direct generation of all-optical random numbers from optical amplitude chaos," *Optics Express*, Vol. 20, No. 4, pp. 4297-4308 (2012).  
 [11] Y. Zhang, J. Zhang, M. Zhang, and Y. Wang, "2.87-Gb/s random bit generation based on bandwidth-enhanced chaotic laser," *Chinese Optics Letters*, Vol. 9, No. 3, pp. 031404 (2011).  
 [12] Y. Akizawa, T. Yamazaki, A. Uchida, T. Harayama, S. Sunada, K. Arai, K. Yoshimura, and P. Davis, "Fast random number generation with bandwidth-enhanced chaotic semiconductor lasers at  $8 \times 50$  Gb/s," *IEEE Photonics Technology Letters*, Vol. 24, No. 12, pp. 1042-1044 (2012).  
 [13] T. Harayama, S. Sunada, K. Yoshimura, J. Muramatsu, K. Arai, A. Uchida, and P. Davis, "Theory of fast nondeterministic physical random-bit generation with chaotic lasers," *Physical Review E*, Vol. 85, No. 4, pp. 046215-1-9 (2012).  
 [14] A. Argyris, M. Hamacher, K. E. Chlouverakis, A. Bogris, and D. Syvridis, "Photonic Integrated Device for Chaos Applications in Communications," *Physical Review Letters*, Vol. 100, No. 19, pp. 194101-1-4 (2008).  
 [15] J. Sacher, W. Elsässer, and E. O. Göbel, "Intermittency in the Coherence Collapse of a Semiconductor Laser with External Feedback," *Physical Review Letters*, Vol. 63, No. 20, pp. 2224-2227 (1989).  
 [16] T. Heil, I. Fischer, and W. Elsässer, "Dynamics of Semiconductor Lasers Subject to Delayed Optical Feedback: The Short Cavity Regime," *Physical Review Letters*, Vol. 87, No. 24, pp. 243901-1-4 (2001).  
 [17] R. Takahashi, Y. Akizawa, T. Yamazaki, A. Uchida, T. Harayama, K. Tsuzuki, S. Sunada, K. Yoshimura, K. Arai, and P. Davis, "Random number generation with a photonic integrated circuit for fast chaos generation," *Proceedings of Nonlinear Theory and Its Applications 2012 (NOLTA 2012)*, (2012).